

Linear and Nonlinear Acoustic Behaviour of Outlet Nozzles

W. H. Moase, M. J. Brear and C. Manzie

Department of Mechanical & Manufacturing Engineering
The University of Melbourne, VIC, 3010 AUSTRALIA

Abstract

The response of outlet nozzles to upstream flow perturbations of varying magnitudes is investigated by numerically solving the quasi-one-dimensional Euler equations. Results are compared to the analytic linear solutions of Marble & Candel for compact and finite length choked nozzles, and those of Rienstra for open nozzles. It is demonstrated that the nonlinear response of the choked exit nozzle is very close to the linear analytic response at forcing amplitudes that are representative of those observed in combustors experiencing limit cycle, thermoacoustic instability. Although jet formation at an open end cannot be represented by quasi-one-dimensional flow, the numerical simulations suggest that the behaviour is slightly more nonlinear than for a choked outlet at the same forcing magnitudes, but still closely in agreement with the analytic linear solutions.

Introduction

Whenever combustion occurs in a duct, coupling between the flame and the duct acoustics can result in unstable behaviour often referred to as 'thermoacoustic' instability. Under many circumstances, the amplitude of the limit cycles can be large enough to cause flame blowout, structural damage, or unacceptable noise. The feedback process between the acoustic disturbances produced by the flame and the acoustic excitation of the flame involves the reflection of disturbances off the outlet of the combustor, which is typically a choked nozzle. In the case of experimental test rigs, it is not always possible for the outlet of the combustor to be choked and instead it is common to have an open outlet exhausting into a large plenum.

Marble & Candel [5] determined the linear response of both compact and finite length choked nozzles. Stow et al. [7] developed theory and performed numerical simulations of the linearised Euler equations for an annular duct, showing that, even in the three-dimensional case, Marble & Candel's analysis for compact nozzles still holds. In their analysis of finite length choked nozzles, Marble & Candel assumed the stream-wise velocity profile of the steady part of the flow throughout the nozzle is linearly distributed. Stow et al. offered an alternative low-frequency asymptotic analysis for finite length nozzles which allows for an arbitrary stream-wise steady velocity profile and also for the difference between finite length and compact nozzle responses to be approximated as an end-correction. Rienstra [6] performed an extensive low Strouhal number asymptotic analysis for the linear acoustic behaviour of an open outlet.

In a typical thermoacoustic limit cycle, the amplitude of the pressure perturbations can be 10% of the mean pressure [3]. Under such conditions it is useful to know whether the assumptions of linearity made by Marble & Candel [5], Stow et al [7] and Rienstra [6] are still valid. The purpose of this paper is therefore to investigate the response of an outlet nozzle to varying amplitude disturbances in order to determine the validity of a linear analysis under conditions when, for example, a combustor is in a limit cycle. The response of the outlet nozzle to upstream flow perturbations is determined by numerically solving the nonlinear quasi-one-dimensional Euler equations. As

this paper is primarily concerned with the effect of a small disturbance assumption, comparison is only made with Marble & Candel's and Rienstra's analyses for choked and open outlets respectively. It is demonstrated that, even for relatively large amplitude disturbances, the response can be accurately represented by these linear boundary conditions.

Theory

Neglecting diffusive and viscous effects, the system is governed by the continuity, Euler (momentum) and energy equations. In this paper, a quasi-one-dimensional form is used

$$\frac{\partial \rho}{\partial t} = -\frac{\partial u \rho}{\partial x} - \rho u \left(\frac{1}{A} \frac{dA}{dx} \right), \quad (1)$$

$$\frac{\partial u}{\partial t} = -u \frac{\partial u}{\partial x} - \frac{1}{\rho} \frac{\partial p}{\partial x}, \quad (2)$$

$$\frac{\partial p}{\partial t} = -u \frac{\partial p}{\partial x} - \gamma p \frac{\partial u}{\partial x} - \gamma p u \left(\frac{1}{A} \frac{dA}{dx} \right), \quad (3)$$

where p is the pressure, u the velocity, ρ the density, and A the cross-sectional area.

Linearisation of the Equations of Motion

A given flow property $G(x, t)$, may be split into its steady-flow value $\bar{G}(x)$ and a perturbation $G'(x, t)$. The Euler equations can then be linearised to first-order in the perturbation quantities. In a region of spatially uniform steady flow, assuming disturbances with time dependence $\exp(i\omega t)$ this gives

$$\frac{p'}{\gamma \bar{p}} = \left[P^+ e^{-i\omega x/(\bar{u} + \bar{c})} + P^- e^{-i\omega x/(\bar{u} - \bar{c})} \right] e^{i\omega t}, \quad (4)$$

$$\frac{u'}{\bar{c}} = \left[P^+ e^{-i\omega x/(\bar{u} + \bar{c})} - P^- e^{-i\omega x/(\bar{u} - \bar{c})} \right] e^{i\omega t}, \quad (5)$$

$$\frac{s'}{c_p} = \frac{p'}{\gamma \bar{p}} - \frac{\rho'}{\bar{\rho}} = \left[\sigma e^{-i\omega x/\bar{u}} \right] e^{i\omega t}, \quad (6)$$

where c is the speed of sound and s is the entropy. So to first-order the unsteady field is composed of three characteristics: a pressure wave P^- traveling upstream at the speed of sound relative to the steady flow; a pressure wave P^+ traveling downstream at the speed of sound relative to the steady flow; and an entropy disturbance σ convecting with the steady flow. In fact, even in spatially non-uniform flow, it can be shown that the entropy disturbances convect at the *local* flow velocity without change. In other words s'/c_p is purely a function of $t - \int dx/\bar{u}$.

Compact Choked Nozzle

A nozzle can be considered compact if it has no storage capacity. Taking the nozzle entrance to be the origin of the system, this means that at $x = 0$, $M' = 0$ if the nozzle is choked at the throat. The Mach number perturbation can be expressed in terms of the pressure, velocity and density fluctuations to give

$$\frac{p'}{\bar{p}} = 2 \frac{u'}{\bar{u}} + \frac{\rho'}{\bar{\rho}}. \quad (7)$$

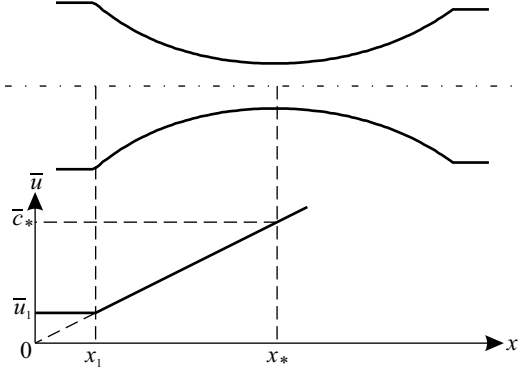


Figure 1: Relationship between choked nozzle geometry and steady velocity distribution.

This is Marble & Candel's [5] well known boundary condition for a compact choked nozzle. Substitution of equations (4)–(6) into (7) yields expressions for the reflection coefficients R_s and R_p , the amplitude of the reflected upstream traveling pressure wave due to incoming entropy and pressure disturbances respectively

$$\frac{P^-}{\sigma} = R_s = \frac{\bar{M}}{2 + (\gamma - 1)\bar{M}}, \quad (8)$$

$$\frac{P^-}{P^+} = R_p = \frac{2 - (\gamma - 1)\bar{M}}{2 + (\gamma - 1)\bar{M}}. \quad (9)$$

Choked Nozzle of Finite Length

In a finite length nozzle, it is not correct to assume that there is zero storage capacity and that the steady flow field is uniform. The analysis must start back at the linearised Euler equations. To ease the algebraic burden of solving the linearised Euler equations, Marble & Candel [5] assume that the steady part of the velocity profile throughout the nozzle increases linearly with position. Furthermore, the origin of the co-ordinate system will no longer be considered the start of the nozzle. Instead, $x = 0$ is the location where the extrapolated nozzle steady velocity profile reaches zero. Subscript 1 designates quantities at the nozzle entrance, and subscript * designates quantities at the nozzle throat. Thus the nozzle length is $x_* - x_1$. The relationship between the nozzle geometry and steady velocity is illustrated in figure 1. For convenience, Marble & Candel also introduce the non-dimensional time $\tau = \bar{c}_* t / x_*$, non-dimensional position $\xi = (x/x_*)^2$ and reduced frequency $\Omega = x_* \omega / \bar{c}_*$ where the excitation frequency is ω . For periodic disturbances,

$$\frac{p'}{\gamma \bar{p}} = P(\xi) \exp(i\Omega\tau), \quad (10)$$

$$\frac{u'}{\bar{u}} = U(\xi) \exp(i\Omega\tau), \quad (11)$$

$$\frac{s'}{c_p} = \sigma \exp\left(i\Omega \left[\tau - \ln \sqrt{\xi/\xi_1} \right] \right). \quad (12)$$

Substituting equations (10)–(12) into the linearised Euler equations gives

$$\xi(1 - \xi) \frac{d^2 P}{d\xi^2} - \left[2 + \frac{2i\Omega}{\gamma + 1} \right] \xi \frac{dP}{d\xi} - \frac{i\Omega(2 + i\Omega)}{2(\gamma + 1)} P = -\frac{i\sigma\Omega}{2(\gamma + 1)} \left(\frac{\xi}{\xi_1} \right)^{-i\Omega/2}, \quad (13)$$

$$(2 + i\Omega)U = -(\gamma + 1)(1 - \xi) \frac{dP}{d\xi} + \sigma \left(\frac{\xi}{\xi_1} \right)^{-i\Omega/2}. \quad (14)$$

Equation (14) can give $U(\xi)$ if $P(\xi)$ is known. P can be found by solution of equation (13) which is of the hypergeometric form — a unique solution can only exist if more information is known about the problem. The pressure disturbance is regular at the nozzle throat, but the location $\xi = 0$ occurs before the nozzle inlet and is out of the domain of interest for this problem. Thus it doesn't matter if a singularity in the solution occurs at $\xi = 0$. Using this information, it is possible to find both a particular $P_p(\xi)$ and homogeneous $P_h(\xi)$ solution to equation (13) such that $P = P_p + kP_h$, where k is a constant, and each solution has the form

$$\sum_{n=0}^{\infty} a_n (1 - \xi)^{n+m}. \quad (15)$$

In order to find k it is necessary to couple the solution to the wave system of the approaching flow. As the flow approaching the nozzle is spatially uniform, equations (4)–(6) hold, giving

$$U(\xi_1) = (2P_1^+ - P(\xi_1)) / \bar{M}_1, \quad (16)$$

so given the magnitudes of the incoming pressure wave P_1^+ and the entropy disturbance σ , equation (16) can be substituted into (14) to close the solution for $P(\xi)$.

Open Outlet

In practice, the exhaust from an open outlet forms a jet. The acoustic interaction with the shear layer of the jet separating from the outlet cannot be modelled with a quasi-one-dimensional analysis. Rienstra [6] provides an extensive low Strouhal number asymptotic analysis of the flow and, in comparison with experiments, concludes that the employment of a Kutta condition at the trailing edge of the pipe outlet is essential in accurately determining the acoustics both within and outside the duct. For zero Strouhal number flow, Rienstra's analysis gives a pressure reflection coefficient of -1 , accurate to first-order in the flow perturbations. In the absence of a Kutta condition, to first-order, Rienstra gives the same pressure reflection coefficient as that given by a simple application of the one-dimensional mass, momentum and energy conservation laws:

$$R_p = -(1 + \bar{M}) / (1 - \bar{M}). \quad (17)$$

Comparison of this reflection coefficient with numerical simulations of the nonlinear quasi-one-dimensional Euler equations may shed some light on the nonlinear effect of high amplitude disturbances on an open outlet when the Kutta condition is employed.

Numerical Solver

The quasi-one-dimensional Euler equations were solved using fourth-order Runge–Kutta time-stepping and a fourth-order Padé spatial finite differencing scheme. These schemes have very small inherent dissipation and give a highly accurate representation of wave propagation [4]. System excitation was caused by sinusoidally varying the relevant outgoing characteristic at the inflow boundary. The system inflow boundary was placed very close to the nozzle entrance so that the nonlinear propagation of the excitation characteristic from inflow boundary to nozzle entrance was negligible. Simulations were run for sufficiently long periods of time to ensure that transients were not present in the final results.

A common source of error in numerical acoustics is the artificial reflection of disturbances from the system boundaries. In the absence of spurious disturbances, boundary conditions that

are nonreflecting in the linear characteristics are given by Giles [2]. As spurious waves can travel at speeds that are significantly different to those of physical waves, a scheme as basic as Giles' can cause reflection of spurious waves. For this reason, discretely nonreflecting boundary conditions were employed as given by Colonius [1]. The chosen scheme was third-order accurate about the Nyquist frequency (spurious) and fourth-order accurate about the steady state (physical) for incoming waves, and fifth-order accurate about the Nyquist frequency for outgoing waves. The chosen boundary conditions resulted in very small reflection of all spurious and physical waves present in typical simulations.

The numerical scheme was validated by solving a number of model problems including the linear propagation of small magnitude waves, and nonlinear wave steepening in large pressure wave propagation. These simulations conformed well with theoretical predictions. The close agreement between the results given by the numerical solver for small amplitude disturbances and the linear analytic solutions presented in this paper is in itself a convincing validation. Initial tests were performed using a number of grid densities and boundary locations. The results were independent of boundary location and converged with increasing grid density. For typical simulations, it was necessary to use around 1000 data points to gain a well resolved solution.

Discussion

Measurement of the linear characteristics in a nonlinear system can be achieved by re-casting equations (4)–(6) in terms of the characteristics to give the following definitions

$$p^+(x,t) = \frac{1}{2} \left(\frac{p'}{\gamma\bar{p}} + \frac{u'}{\bar{c}} \right), \quad (18)$$

$$p^-(x,t) = \frac{1}{2} \left(\frac{p'}{\gamma\bar{p}} - \frac{u'}{\bar{c}} \right), \quad (19)$$

$$\frac{s'}{c_p}(x,t) = \frac{p'}{\gamma\bar{p}} - \frac{p'}{\bar{p}}. \quad (20)$$

As already mentioned, the excitation characteristic is sinusoidal in time. In a linear system, that would mean that the pressure wave reflected from the nozzle is also sinusoidal. However, the temporal nature of the reflected pressure wave may be different for a nonlinear system. A question then arises as how to measure its magnitude. At the nozzle inlet, it is easy to take a full steady state period of the reflected pressure wave $p_{ss}^-(t)$, and its Fourier transform \mathcal{F} . The magnitude of the response can be considered the Fourier component occurring at the excitation frequency, \mathcal{F}_ω . The nonlinearity is indicated by the difference between the output and its mode occurring at the excitation frequency. In a normalised form, this can be expressed as

$$\kappa = \frac{||\mathcal{F}_\omega| \cos(2\pi\omega t + \arg(\mathcal{F}_\omega)) - p_{ss}^-(t)||_2}{|p_{ss}^-(t)|_2}, \quad (21)$$

where $||\cdot||_2$ denotes the ℓ^2 -norm. When $\kappa = 0$, the output signal is sinusoidal at the input frequency which infers a linear response. When $\kappa = 1$, all of the output occurs at frequencies other than the input frequency, suggesting the output is not at all linearly related to the input.

Simulations were performed in order to measure the reflection coefficients R_p and R_s for a 'compact' choked nozzle over a range of Mach numbers. In order to ensure compactness, a value of $\Omega = 0.01$ was used. The results of these simulations are shown in figure 2. Even when the excitation characteristics are as large as 0.1, the numerically determined reflection coefficients are very close to the first-order approximation of Marble & Candel [5]. This was a surprising result and of practical

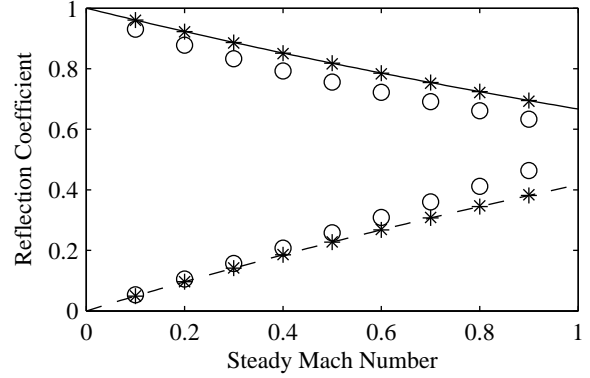


Figure 2: Steady Mach number dependence of the reflection coefficient of a choked exit nozzle with $\Omega = 0.01$. Marble and Candel's compact result for $|R_p|$ in solid line and $|R_s|$ in dashed line. Simulations for: σ , $P^+ = 0.5$ (\circ); σ , $P^+ = 0.1$ (\times); and σ , $P^+ = 0.001$ ($+$).

interest since the pressure perturbations during thermoacoustic limit cycles can be 10% of the steady state pressure. For excitation characteristics of 0.5, a significant deviation from the linear approximation is evident, although perturbations of this magnitude are unlikely to occur in thermoacoustic limit cycles.

Further simulations were performed to measure the effect of finite nozzle length on R_s for a choked exit with a steady approach Mach number of 0.61 (the same Mach number as that studied by Marble & Candel [5]). Care was taken to ensure that the geometry enforced a linear steady velocity profile along the nozzle. Figure 3 shows a Bode plot of the entropy reflection coefficient for a finite length nozzle. It is clearly observed that the effect of finite nozzle length is to filter out the reflection of high frequency oscillations. This indicates that in the stability analysis of many real systems with a choked outlet nozzle, only the low frequency modes of vibration are of interest. Again the agreement between Marble & Candel's first-order approximation and the numerical results is surprising, even for $\sigma = 0.1$. Shown below the Bode plot is the nonlinearity measure κ . Although the higher amplitude excitation still gives a similar reflection coefficient to the linear model, some small nonlinearity is detected in the waveform of the response. Figure 4 gives an example of the degree of nonlinearity observed by comparing $p^-(t)$ at the nozzle entrance to its component at the excitation frequency with $\kappa = 0.05$. Note that the time-averaged value of the nonlinear perturbation is non-zero.

Numerical simulations were also performed for the quasi-one-dimensional flow through an open outlet. The open geometry was represented by a smooth fractional area change of 100 occurring over a length of 0.005 of the incoming wavelength. This ensured that the outlet was both compact and emptying into an approximately infinite plenum. As discussed earlier in this paper, such a flow is not physical due to separation of the flow from the outlet, and formation of a jet. Nonetheless, figure 5 compares the linear analytic expression to those found numerically. The agreement between the numerical simulations and the analytical results for R_p is good, although the open outlet is slightly more nonlinear than the choked outlet.

Conclusions

The Euler equations have been solved numerically for the case of quasi-one-dimensional flow through outlet nozzles. The reflection coefficients have been found for open, compact choked and finite length choked nozzles. For perturbation amplitudes

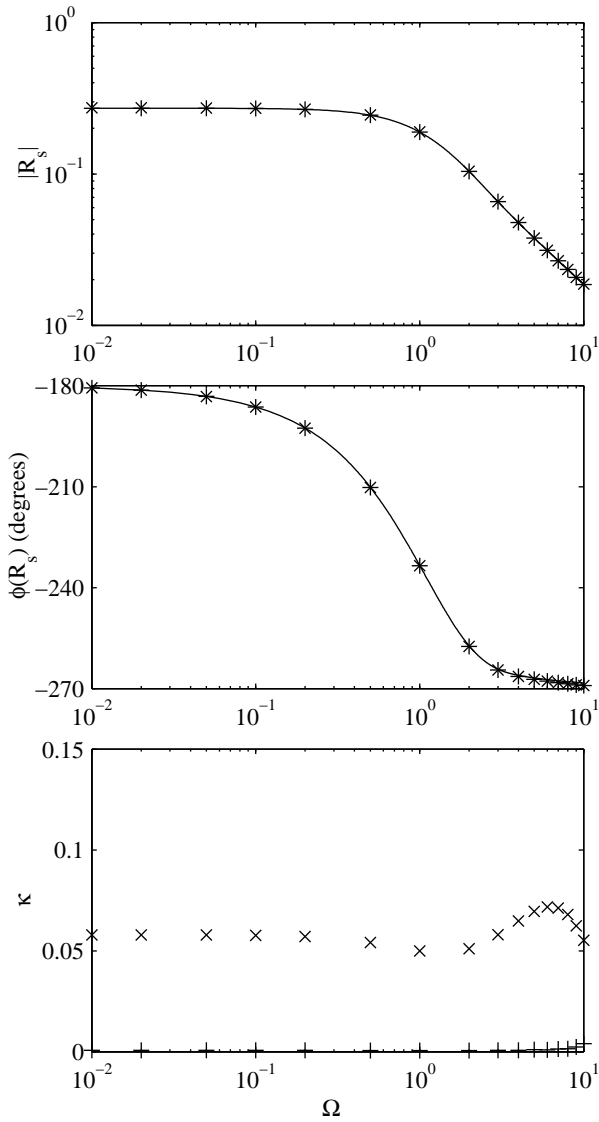


Figure 3: Reduced frequency dependence of entropy reflection coefficient of a choked nozzle with $\bar{M} = 0.61$. Solid line: Marble and Candel's finite length result. Simulations for: $\sigma = 0.1$ (\times); and $\sigma = 0.001$ ($+$).

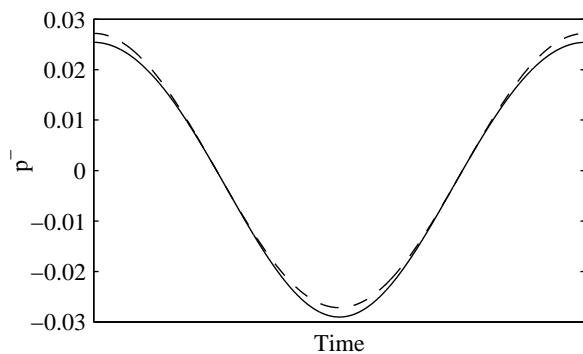


Figure 4: Reflected pressure wave from a choked exit nozzle as a function of time. Actual waveform shown in solid line, and its Fourier component at the excitation frequency shown in dashed line. $\bar{M} = 0.61$, $\Omega = 0.1$ & $\sigma = 0.1$.

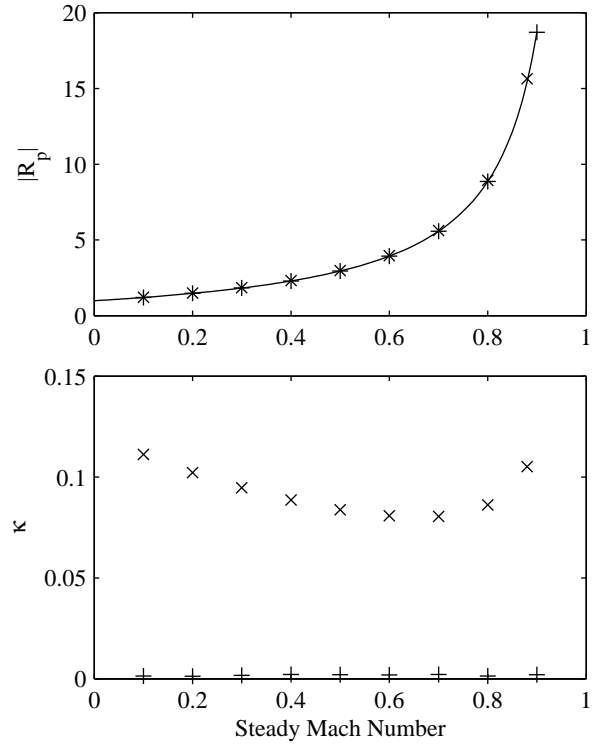


Figure 5: Dependence of reflection coefficient on steady Mach number. Analytical linear result in solid line. Simulations for: $P^- = 0.001$ ($+$); and $P^- = 0.1$ (\times).

as big as 10% of their corresponding steady flow quantities, a small non-linearity is observed, but the reflection coefficients are very closely represented by linear approximations. This suggests that in the analysis of typical thermoacoustic limit cycles, the outlet will be close to linear and the boundary conditions of Marble & Candel as well as Rienstra are applicable.

References

- [1] Colonius, T., Numerically Nonreflecting Boundary and Interface Conditions for Compressible Flow and Aeroacoustic Computations, *AIAA Journal*, **35**, 1997, 1126–1133.
- [2] Giles, M.B., Nonreflecting Boundary Conditions for Euler Equation Calculations, *AIAA Journal*, **28**, 1990, 2050–2058.
- [3] Langhorne, P.J., Reheat Buzz: an Acoustically Coupled Combustion Instability. Part I: Experiment, *J. Fluid Mech.*, **193**, 1988, 417–443.
- [4] Lele, S.K., Compact Finite Difference Schemes with Spectral-Like Resolution, *J. Comput. Phys.*, **103**, 1992, 16–42.
- [5] Marble, F.E. and Candel, S.M., Acoustic Disturbance from Gas Non-Uniformities Convected Through a Nozzle, *J. Sound Vib.*, **55**, 1977, 225–243.
- [6] Rienstra, S.W., A Small Strouhal Number Analysis for Acoustic Wave-Jet Flow-Pipe Interaction, *J. Sound Vib.*, **86**, 1983, 539–556.
- [7] Stow, S.R., Dowling, A.P. and Hynes, T.P., Reflection of Circumferential Modes in a Choked Nozzle, *J. Fluid Mech.*, **467**, 2002, 215–239.